

## Articles

# Self-Contained, Fully Integrated Biochip for Sample Preparation, Polymerase Chain Reaction Amplification, and DNA Microarray Detection

Robin Hui Liu,<sup>\*,†</sup> Jianing Yang,<sup>†</sup> Ralf Lenigk,<sup>†</sup> Justin Bonanno,<sup>†</sup> and Piotr Grodzinski<sup>\*,‡</sup>

Microfluidics Laboratory, Motorola Labs, Tempe, Arizona 85284

**A fully integrated biochip device that consists of microfluidic mixers, valves, pumps, channels, chambers, heaters, and DNA microarray sensors was developed to perform DNA analysis of complex biological sample solutions. Sample preparation (including magnetic bead-based cell capture, cell preconcentration and purification, and cell lysis), polymerase chain reaction, DNA hybridization, and electrochemical detection were performed in this fully automated and miniature device. Cavitation microstreaming was implemented to enhance target cell capture from whole blood samples using immunomagnetic beads and accelerate DNA hybridization reaction. Thermally actuated paraffin-based microvalves were developed to regulate flows. Electrochemical pumps and thermopneumatic pumps were integrated on the chip to provide pumping of liquid solutions. The device is completely self-contained: no external pressure sources, fluid storage, mechanical pumps, or valves are necessary for fluid manipulation, thus eliminating possible sample contamination and simplifying device operation. Pathogenic bacteria detection from approximately milliliters of whole blood samples and single-nucleotide polymorphism analysis directly from diluted blood were demonstrated. The device provides a cost-effective solution to direct sample-to-answer genetic analysis and thus has a potential impact in the fields of point-of-care genetic analysis, environmental testing, and biological warfare agent detection.**

A fully integrated biochip needs to perform all functions including sample preparation, mixing steps, chemical reactions, and detection in a miniature fluidic device. Most of the currently demonstrated microfluidic or microarray devices pursue single functionality and use purified DNA or homogeneous sample as an input sample. On the other hand, practical applications in clinical and environmental analysis require processing of samples as complex and heterogeneous as whole blood or contaminated environmental fluids. Due to the complexity of the sample

preparation, most available biochip systems still perform this initial step off-chip using traditional benchtop methods. As a result, rapid developments in back-end detection platforms have shifted the bottleneck, impeding further progress in rapid analysis devices, to front-end sample preparation where the “real” samples are used.

Since the early work of Harrison and co-workers<sup>1</sup> on chip-based capillary electrophoresis (CE), the advances of the microfluidic lab-on-a-chip technologies have been multidirectional and have addressed the following issues: high throughput of the analysis,<sup>2</sup> functional complexity,<sup>3–6</sup> level of integration,<sup>7</sup> on-chip sample preparation,<sup>3,8–10</sup> and low-cost fabrication and manufacturing.<sup>11,12</sup> Several researchers have developed devices allowing for performance of multistep assays using complicated channel networks, while pumps, valves, and detectors were left off-chip and were built into the desktop test station.<sup>8,9,13</sup> Others argued for integrating all functional components into the chip and preferred portable solutions.<sup>14</sup> The latter efforts led to ingenious demonstrations of on-chip valving<sup>7,15,16</sup> and pumping schemes<sup>17–20</sup> in an attempt to depart from traditional microelectromechanical systems ap-

- (1) Harrison, D. J.; Fluri, K.; Seiler, K.; Fan, Z. H.; Effenhauser, C. S.; Manz, A. *Science* **1993**, *261*, 895–897.
- (2) Simpson, P. C.; Roach, D.; Woolley, A. T.; Thorsen, T.; Johnston, R.; Sensabaugh, G. F.; Mathies, R. A. *Proc. Natl. Acad. Sci. U.S.A.* **1998**, *95*, 2256–2261.
- (3) Anderson, R. C.; Su, X.; Bogdan, G. J.; Fenton, J. *Nucleic Acids Res.* **2000**, *28*, e60.
- (4) Lenigk, R.; Liu, R. H.; Athavale, M.; Chen, Z. J.; Ganser, D.; Yang, J. N.; Rauch, C.; Liu, Y. J.; Chan, B.; Yu, H. N.; Ray, M.; Marrero, R.; Grodzinski, P. *Anal. Biochem.* **2002**, *311*, 40–49.
- (5) Taylor, M. T.; Belgrader, P.; Joshi, R.; Kintz, G. A.; Northrup, M. A. *Micro Total Anal. Syst.* **2001**, 670–672.
- (6) Liu, Y. J.; Rauch, C. B.; Stevens, R. L.; Lenigk, R.; Yang, J. N.; Rhine, D. B.; Grodzinski, P. *Anal. Chem.* **2002**, *74*, 3063–3070.
- (7) Thorsen, T.; Maerkl, S. J.; Quake, S. R. *Science* **2002**, *298*, 580–584.
- (8) Yuen, P. K.; Kricka, L. J.; Fortina, P.; Panaro, N. J.; Sakazume, T.; Wilding, P. *Genome Res.* **2001**, *11*, 405–412.
- (9) Khandurina, J.; McKnight, T. E.; Jacobson, S. C.; Waters, L. C.; Foote, R. S.; Ramsey, J. M. *Anal. Chem.* **2000**, *72*, 2995–3000.
- (10) Waters, L. C.; Jacobson, S. C.; Kroutchinina, N.; Khandurina, J.; Foote, R. S.; Ramsey, J. M. *Anal. Chem.* **1998**, *70*, 158–162.
- (11) Whitesides, G. M.; Stroock, A. D. *Phys. Today* **2001**, *54* (6), 42–48.
- (12) Boone, T.; Fan, Z. H.; Hooper, H.; Ricco, A.; Tan, H. D.; Williams, S. *Anal. Chem.* **2002**, *74*, 78A–86A.
- (13) Cheng, J.; Sheldon, E. L.; Wu, L.; Uribe, A.; Gerrue, L. O.; Carrino, J.; Heller, M. J.; O’Connell, J. P. *Nat. Biotechnol.* **1998**, *16*, 541–546.
- (14) Burns, M. A.; Johnson, B. N.; Brahmasandra, S. N.; Handique, K.; Webster, J. R.; Krishnan, M.; Sammarco, T. S.; Man, P. M.; Jones, D.; Heldsinger, D.; Mastrangelo, C. H.; Burke, D. T. *Science* **1998**, *282*, 484–487.

\* To whom correspondence should be addressed. E-mail: RobinHLiu6@yahoo.com; piotrg@lanl.gov.

<sup>†</sup> Current address: Center for Applied NanoBioscience Center, Arizona State University, Tempe, AZ 85287.

<sup>‡</sup> Current address: Los Alamos National Laboratory, Los Alamos, NM 87545.

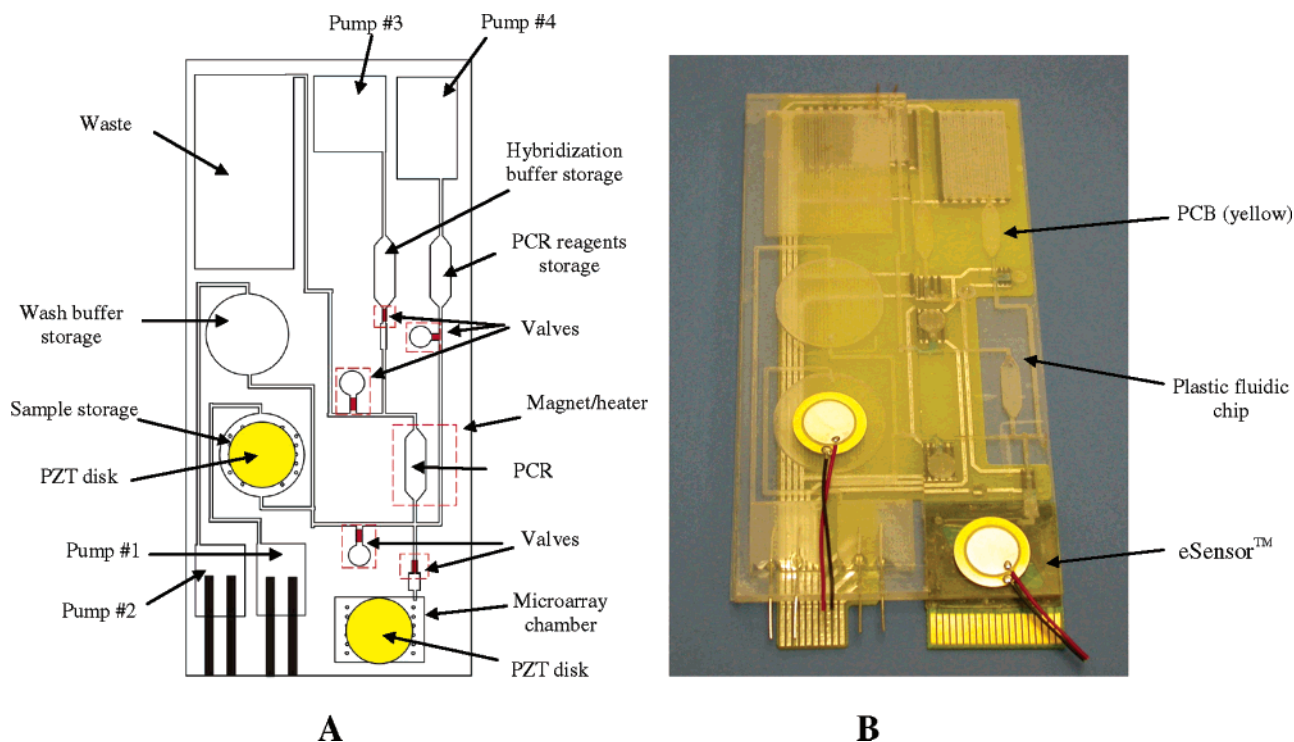


Figure 1. (A) Schematic of the plastic fluidic chip. Pumps 1–3 are electrochemical pumps, and pump 4 is a thermopneumatic pump. (B) Photograph of the integrated device that consists of a plastic fluidic chip, a printed circuit board (PCB), and a Motorola eSensor microarray chip.

proaches that are complicated in fabrication and therefore expensive. Most of the work has been directed toward the integration of DNA amplification with CE,<sup>14,21,22</sup> and there are only few reports on combining sample preparation with polymerase chain reaction (PCR) and DNA microarrays. Anderson et al. reported an integrated system that performed RNA purification from a serum lysate, followed by PCR, serial enzymatic reactions, and nucleic acid hybridization.<sup>3</sup> Yuen et al. reported a microchip module design for blood sample preparation (white blood cell isolation), PCR, and DNA microarray analysis.<sup>8</sup> Lack of efficient, yet simple in design, on-chip mixing, valving, and pumping techniques and the use of optical-based microarray detection make the above systems less desirable for applications valuing portable solutions such as point-of-care diagnostics, in-field environmental testing, and on-site forensics.

We have recently developed an integrated biochip device that integrated sample preparation with PCR and DNA microarray.<sup>23</sup> In this paper, we report on the development of an optimized self-contained and fully integrated biochip device for sample-to-answer

DNA analysis. The on-chip analysis starts with the preparation process of a whole blood sample, which includes magnetic bead-based target cell capture, cell preconcentration and purification, and cell lysis, followed by PCR amplification and electrochemical microarray-based detection. The biochip design and developments of the key microfluidic components, such as mixers, valves, and pumps, are described. Pathogenic bacteria detection from milliliters of whole blood samples and single-nucleotide polymorphism analysis directly from blood samples are presented.

## EXPERIMENTAL SECTION

**Device Design and Fabrication.** The biochip device (Figure 1) consists of a plastic chip, a printed circuit board (PCB), and a Motorola eSensor microarray chip. The plastic chip includes a mixing unit for rare cell capture using immunomagnetic separation, a cell preconcentration/purification/lysis/PCR unit, and a DNA microarray chamber. The complexity of the chip design is minimized by using some of the chambers for more than one function. For example, the chamber to capture and preconcentrate target cells is also used for subsequent cell lysis and PCR. The PCB consists of embedded resistive heaters and control circuitry. The Motorola eSensor (Motorola Inc., Pasadena, CA) is a separate PCB substrate with  $4 \times 4$  gold electrodes on which thiol-terminated DNA oligonucleotides are immobilized via self-assembly to detect electrochemical signals of hybridized target DNA.<sup>24,25</sup>

The operation of the biochip device is as follows. A biological sample (such as a blood solution) and a solution containing

- (15) Beebe, D. J.; Moore, J. S.; Bauer, J. M.; Yu, Q.; Liu, R. H.; Devadoss, C.; Jo, B.-H. *Nature* **2000**, *404*, 588–590.
- (16) Liu, R. H.; Yu, Q.; Beebe, D. J. *J. Microelectromech. Syst.* **2002**, *11*, 45–53.
- (17) Zeng, S. L.; Chen, C. H.; Santiago, J. G.; Chen, J. R.; Zare, R. N.; Tripp, J. A.; Svec, F.; Frechet, J. M. J. *Sens. Actuators, B* **2002**, *82*, 209–212.
- (18) Dodson, J. M.; Feldstein, M. J.; Leatzow, D. M.; Flack, L. K.; Golden, J. P.; Ligler, F. S. *Anal. Chem.* **2001**, *73*, 3776–3780.
- (19) Tsai, J. H.; Lin, L. W. *J. Microelectromech. Syst.* **2002**, *11*, 665–671.
- (20) Bohm, S.; Olthuis, W.; Bergveld, P. *Sens. Actuators, A* **1999**, *77*, 223–228.
- (21) Waters, L. C.; Jacobson, S. C.; Kroutchinina, N.; Khandurina, J.; Foote, R. S.; Ramsey, J. M. *Anal. Chem.* **1998**, *70*, 158–162.
- (22) Woollery, A. T.; Hadley, D.; Landre, P.; deMello, A. J.; Mathies, R. A.; Northrup, M. A. *Anal. Chem.* **1996**, *68*, 4081–4086.
- (23) Liu, R. H.; Yang, J.; Lenigk, R.; Bonanno, J.; Grodzinski, P.; Zenhausern, F. *Proc. Micro-TAS 2003*, Squaw Valley, CA, Oct. 5–9, 2003, 2003; pp 1319–1322.

(24) Farkas, D. H. *Clin. Chem.* **2001**, *47*, 1871–1872.

(25) Umek, R. M.; Lin, S. W.; Vielmetter, J.; Terbruggen, R. H.; Irvine, B.; Yu, C. J.; Kayyem, J. F.; Yowanto, H.; Blackburn, G. F.; Farkas, D. H.; Chen, Y. P. *J. Mol. Diagn.* **2001**, *3*, 74–84.

immunomagnetic capture beads are loaded in the sample storage chamber. Other solutions including a wash buffer, PCR reagents, and hybridization buffer are separately loaded in other storage chambers. The biochip device is then inserted into an instrument, which provides electrical power, PCR thermal cycling, DNA electrochemical signal readout, and magnetic elements for bead arrest. The PCR chamber of the plastic chip is sandwiched between a Peltier heating element (Melcor Corp., Trenton, NJ) and a permanent magnet. The on-chip sample preparation starts with a mixing and incubation step in the sample storage chamber to ensure target cell capture from the blood using immunomagnetic capture beads. The sample mixture is then pumped through the PCR chamber, where target cell capture and preconcentration occur as the bead–bacteria conjugates are trapped by the magnet. The washing buffer is subsequently pumped through the PCR chamber to purify the captured cells. After the PCR reagents are transferred into the PCR chamber, all the normally open microvalves surrounding the chamber are closed, and thermal cell lysis and PCR are performed. Once PCR is completed, the normally closed microvalves are opened, allowing the hybridization buffer and the PCR product to be pumped into the detection chamber, where acoustic mixing of the target and DNA hybridization reaction occurs. The electrochemical hybridization signals corresponding to the redox reaction of the ferrocene-labeled signaling probes that hybridize with the target DNA bound to the immobilized probes are detected on the chip and recorded by the instrument.

The plastic chip measures  $60 \times 100 \times 2$  mm and has channels and chambers that range from  $300 \mu\text{m}$  to 1.2 mm in depth and 1 to 5 mm in width. The plastic chip was machined in a polycarbonate (PC) substrate (1.5 mm thick) using conventional computer-controlled machining (Prolight 2500, Intelitek Inc., Manchester, NH), followed by sealing it with a thin PC cover layer ( $500 \mu\text{m}$  thick) using a solvent-assistant thermal bonding technique. During the bonding process, acetone was first applied on one side of the thin cover layer. After 1 min, the cover layer with the gluey surface caused by the chemical reaction with acetone was bonded on the substrate plastic layer followed by a press of 1-ton force at  $385^\circ\text{F}$  for 2 min in a hydraulic press (Carver, Inc., Wabash, IN). Platinum wires with 0.5-mm diameter were inserted into the electrochemical pumping chambers, which were then loaded with  $20 \mu\text{L}$  of 5 M NaCl solutions to form electrochemical pumps. Two piezoelectric disks (each 15-mm diameter, APC Inc., Mackeyville, PA) that were used to provide acoustic micromixing were bonded onto the external surfaces of the sample storage chamber and the microarray detection chamber, respectively, using a super glue (Duro, Loctite Corp., Avon, OH). Fabrication of the paraffin-based microvalves in the biochip began with heating the plastic chip using a hot plate with a temperature of  $90^\circ\text{C}$  that is above the melting temperature of the paraffin. Solid paraffin ( $\sim 10$  mg) with a melting temperature  $T_m$  of  $70^\circ\text{C}$  was then placed into each of the paraffin access holes on the plastic chip. The paraffin was melted instantaneously, and capillary force drove the molten paraffin into the channels. The chip was then removed from the hot plate. The paraffin solidified, resulting in an array of microvalves in the device. The paraffin access holes were subsequently sealed using an adhesive tape (Adhesive Research Inc., Glen Rock, PA). The plastic chip was then bonded with the PCB using a

double-sided adhesive tape (Adhesive Research Inc., Glen Rock, PA). The eSensor microarray chip was attached to the detection cavity of the plastic chip using a double-sided adhesive tape.

**Pathogenic Bacteria Detection.** Pathogenic bacteria detection from a whole blood sample was performed using the described device. *Escherichia coli* K12 cells inoculated in a whole rabbit blood were used as a model for demonstration. The input sample is 1 mL of whole citrated rabbit blood (Colorado Serum Co., Denver, CO) containing  $10^3$ – $10^6$  *E. coli* K12 cells. Ten microliters of biotinylated polyclonal rabbit-anti-*E. coli* antibody (ViroStat, Portland, ME) and  $20 \mu\text{L}$  of streptavidin-labeled Dynabeads (total  $1.3 \times 10^7$  M-280 beads, Dynal Biotech, Inc., Lake Success, NY) were also added into the sample storage chamber. The bead–antibody–*E. coli* cell complexes were formed during a 20-min cavitation microstreaming-based mixing period. Following the mixing, the blood sample mixture was pumped using an electrochemical pump (pump 1 in Figure 1A) at 0.1 mL/min into the PCR chamber, where the beads–antibody–cells complexes were collected by the magnet. The uncaptured samples were flowed into the waste chamber. Subsequently, 1 mL of wash buffer was pumped at 0.1 mL/min through the PCR chamber using pump 2 to wash the captured complexes.

As a result of the cell preconcentration and purification steps, the purified bead–antibody–cell complexes were isolated from the blood sample solution and trapped in the PCR chamber. Following influx of the PCR reagents to the PCR chamber and closing of all the paraffin-based valves, thermal cell lysis and two-primer asymmetric PCR were performed to amplify an *E. coli* K12-specific gene fragment and achieve single-stranded DNA amplicon in the presence of beads. A pair of *E. coli* K12-specific primers were used to amplify a 221-bp *E. coli* K12-specific gene (MG1655) fragment, with forward primer, 5' AAC GGC CAT CAA CAT CGA ATA CAT 3', and reverse primer, 5' GGC GTT ATC CCC AGT TTT TAG TGA 3'. The PCR reaction mixture ( $20 \mu\text{L}$ ) consists of Tris-HCl (pH 8.3) 10 mM, KCl 50 mM,  $\text{MgCl}_2$  2 mM, gelatin 0.001%, dNTPs 0.4 mM each, bovine serum albumin 0.1%, forward primer 0.05  $\mu\text{M}$ , reverse primer 5  $\mu\text{M}$ , and AmpliTaq DNA polymerase (Applied Biosystems, Foster City, CA) 5 units. The PCR was performed with an initial denature step at  $94^\circ\text{C}$  for 4 min followed by 35 cycles of  $94^\circ\text{C}$  for 45 s,  $55^\circ\text{C}$  for 45 s, and  $72^\circ\text{C}$  for 45 s, with a final extension at  $72^\circ\text{C}$  for 3 min. As a control, asymmetric PCR was also run in parallel in a conventional DNA Engine thermal cycler (MJ Research Inc., South San Francisco, CA) with the same volume and assay conditions.

Following the PCR, two paraffin-based microvalves, one regulating the channel between the PCR chamber and the hybridization buffer storage chamber and the other one between the PCR and the microarray chamber, were opened. The PCR products were then transported to the eSensor microarray chamber along with hybridization buffer ( $20 \mu\text{L}$ ) using pump 3 as shown in Figure 1A. The hybridization buffer contains  $1 \times$  hybridization buffer stock, 7% fetal calf serum, 1 mM hexanethiol, and 0.5  $\mu\text{M}$  signaling probe.<sup>24,25</sup> The microarray chamber was incubated at  $35^\circ\text{C}$ , and the electrochemical signals from the eSensor microarray were measured at 0 min, 15 min, 30 min, and 1 h. The eSensor devices allow for continuous measurement of DNA hybridization signals during the reaction due to the homogeneous nature of the assay.<sup>24,25</sup> The ac voltammetry



technique to gather the electrochemical signals corresponding to hybridization reaction is described in more detail elsewhere.<sup>24,25</sup>

**Single-Nucleotide Polymorphism Assay.** In addition to bacterial DNA detection, we performed the detection of hematochromatosis-associated single-nucleotide polymorphism (HFE-C) directly from a diluted blood sample in the device. It was shown previously that the eSensor chip was able to discriminate single-base mismatches, using genetic variation associated with hereditary hemochromatosis as a model.<sup>25</sup> Mutations in the HFE gene associated with hematochromatosis are responsible for iron overload and can result in a number of different pathologies.<sup>26</sup> In the assay performed in our integrated device, a mixture of human blood (1.4  $\mu\text{L}$ ) and PCR reagents (total volume 20  $\mu\text{L}$ ) was loaded into the PCR chamber. Thermal cell lysis followed by a multiplexed asymmetric PCR amplification (i.e., 94 °C for 4 min followed by 35 cycles of 94 °C for 45 s, 55 °C for 45 s, and 72 °C for 45 s, with a final extension at 72 °C for 3 min) was performed to simultaneously amplify DNA sequences containing the sites for HFE-C polymorphism. The asymmetrical PCR used one set of three primers with a final concentration of 0.5  $\mu\text{M}$  per primer,<sup>27</sup> 400  $\mu\text{M}$  dNTP, 50 mM KC, 10 mM Tris-HCL (pH 8.3), 2 mM  $\text{MgCl}_2$ , 0.05 U/ $\mu\text{L}$  *Taq* polymerase, and 100  $\mu\text{g}/\text{mL}$  bovine serum albumin. Once PCR was completed and the valves were opened, the hybridization buffer (20  $\mu\text{L}$ , Motorola Life Sciences, Pasadena, CA) and the amplification product were pumped into the microarray chamber, followed by 1-h hybridization and electrochemical signal scanning.

## RESULT AND DISCUSSION

**Fluidic Transport.** The fluidic architecture takes advantage of the fluid gravity to remove the air bubbles from the system without the use of porous hydrophobic vents.<sup>3</sup> As in many other microfluidic devices, air plugs or bubbles trapped in the system are of great practical concern, because they often lead to difficulties in controlling the flow and hinder uniform mixing between fluids. Since all the chambers have dimensions of  $\geq 500 \mu\text{m}$  and fluid volumes on the order of microliters or milliliters were handled in the system, the Reynolds number for the flow is on the order of 10 or above. As a result, fluid gravity dominated surface forces when the chip was operated in a vertical position. Gas bubbles always migrated to the upper portion of the chamber due to buoyant forces whereas the liquid solution resided in the lower portion. For example, in the PCR chamber where fluids entered at the bottom of the chamber, all air bubbles trapped in the solution escaped toward the top of the chamber and subsequently traveled to the downstream waste chamber, leaving the PCR chamber bubble-free.

**Micromixing.** An important performance aspect of the device is its ability to rapidly mix liquid solutions by means of a cavitation microstreaming technique. Rapid and homogeneous mixing is difficult to achieve in microscale or miniature fluidic systems, where mixing is typically dominated by diffusion. A pure diffusion-based mixing process can be very inefficient, particularly in solutions containing macromolecules or particles that have diffusion coefficients several orders of magnitude lower than that of most liquids. Although many in-line micromixers have been

successfully demonstrated,<sup>28,29</sup> micromixing in chamber devices remains challenging since most conventional chamber micromixers suffer from complicated fabrication and integration and complex operation regime.<sup>30,31</sup>

We have developed a novel micromixing technique based on the principle of cavitation microstreaming.<sup>27,32</sup> A set of air bubbles was trapped inside the solution using air pockets (500  $\mu\text{m}$  in diameter and 500  $\mu\text{m}$  in depth) in the cover layer of the chamber. These bubbles were set into vibration by an acoustic field generated using an external piezoelectric transducer (PZT). The frictional forces generated at the bubble/liquid interface induced bulk fluid circulation around the bubbles, a phenomenon called cavitation microstreaming. The most effective mixing enhancement was provided by pulsation of air bubbles having a size and resonant frequency selected in accordance with the insonation frequency induced by the PZT disk. Fluidic experiments showed that the time taken to achieve a complete mixing in a 50- $\mu\text{L}$  chamber using cavitation microstreaming was significantly reduced from hours (a pure diffusion-based mixing) to only 6 s.<sup>27</sup> Cavitation microstreaming was implemented in the sample storage chamber to enhance mixing and binding of target bacterial cells (*E. coli* K12) inoculated in blood with immunomagnetic capture beads. Cell capture efficiency of 73% was achieved, as compared to 91% using conventional vortexing in a microfuge tube and 2% using pure diffusion in the same chamber microdevice. Cavitation microstreaming was also implemented in the DNA eSensor microarray chamber to enhance the rate of DNA hybridization.<sup>27</sup> Hybridization reaction kinetics study showed that acoustic microstreaming resulted in up to 5-fold kinetics acceleration with significantly improved signal uniformity.

Cavitation microstreaming is an effective solution to the difficult problem of mixing enhancement in a microfluidic or miniaturized fluidic environment, where diffusion plays a dominating role. Conventional DNA microarray hybridization relies on diffusion of DNA target to surface-bound DNA probes and is often a lengthy rate-limiting process (6–20 h). The bulk of the target solution is at a considerable distance, on the molecular length scale, from the reaction site on the chip surface. For example, the diffusion coefficient of a 250-bp DNA fragment in water at room temperature is  $\sim 2 \times 10^{-7} \text{ cm}^2/\text{s}$ , and thus, its diffusion time along a length of 500  $\mu\text{m}$  is  $\sim 100 \text{ min}$ . This inefficient diffusion greatly limits the throughput of sample analyses. Cavitation microstreaming not only provides rapid lateral mass transport of fluidic elements but also enhances the vertical mass transport of target DNA in the solution toward the DNA probes on the chip surface. The combination of rapid lateral and vertical fluid movements results in rapid transport of targets in solution to the diffusion boundary layer and thus allows for continuous replenishment of fresh DNA targets around the probes that has been depleted of complementary targets. As a result, the hybridization rate is enhanced and so is the hybridization uniformity across the chip. Moreover, cavitation

(26) Press, R. D. *Arch. Pathol. Lab. Med.* **1999**, *123*, 1053–1059.

(27) Liu, R. H.; Lenigk, R.; Yang, J.; Druyor-Sanchez, R.; Grodzinski, P. *Anal. Chem.* **2003**, *75*, 1911–1917.

(28) Stroock, A. D.; Dertinger, S. K. W.; Ajdari, A.; Mezic, I.; Stone, H. A.; Whitesides, G. M. *Science* **2002**, *295*, 647–651.

(29) Liu, R. H.; Stremler, M. A.; Sharp, K. V.; Olsen, M. G.; Santiago, J. G.; Adrian, R. J.; Aref, H.; Beebe, D. J. *J. Microelectromech. Syst.* **2000**, *9*, 190–197.

(30) Moroney, R. M.; White, R. M.; Howe, R. T. *Appl. Phys. Lett.* **1991**, *59*, 774–776.

(31) Zhu, X.; Kim, E. S. *Sens. Actuators, A* **1998**, *66* (1–3), 355–360.

(32) Liu, R. H.; Yang, J.; Pindera, M. Z.; Athavale, M.; Grodzinski, P. *Lab Chip* **2002**, *2* (3), 151–157.

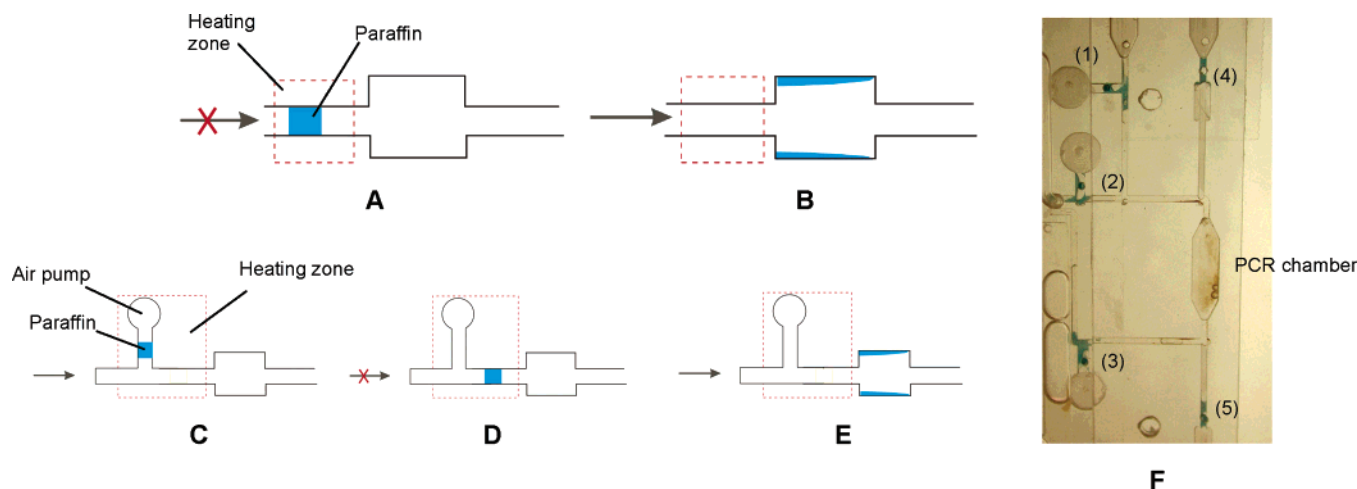


Figure 2. Schematic illustrations of a close-open paraffin microvalve design (A, B) and an open-close-open microvalve design (C–E). The former has a block of paraffin that initially closes the channel (A). To open the channel, the paraffin is melted using the heater underneath and moved downstream by the pressure from the upstream channel. Once the molten paraffin moves out of the heating zone, it starts to solidify on the wall of a wide channel section resulting in an open channel (B). The latter is a normally open valve with a block of paraffin connected to an air pocket that acts as a thermally actuated air pump (C). When the heater is activated, the air in the pocket expands and pushes the molten paraffin into the regulated channel. If the heater is turned off immediately, the paraffin solidifies in the main flow channel, resulting in a closed channel (D). The channel can be reopened by reactivating the heater (E). A photograph (F) of the PCR chamber surrounded by five paraffin-based microvalves: valves 1–3 are open-close valves, and valves 4 and 5 are close-open valves. All valves are in “closed” position prior to initiating PCR. The PCB that provides thermal actuation to the valves is not shown here. Purified *E. coli*-bead complexes (brown) are retained in the PCR chamber.

microstreaming requires a very simple mixing apparatus compared to most existing chamber micromixers<sup>30,31</sup> and thus can be easily implemented in biochip devices. Other advantages of cavitation microstreaming include low power consumption ( $\sim 2$  mW) and low cost.

**Microvalves.** To facilitate a sequential and multistage analysis, a novel microvalving technique has been developed and implemented into the biochip. The choice of an appropriate valving technology is not a trivial task since the simplicity of the design has to be balanced with performance requirements. Most conventional “on-off” microvalves involve a diaphragm coupled with a pneumatic source,<sup>7</sup> a stimuli-sensitive actuator,<sup>15,16</sup> or an electromechanical actuator.<sup>33–36</sup> Not only is the fabrication of such microvalves involving multilayer construction complicated, but their integration into complex microfluidic systems has also proven to be nontrivial. As a result, these conventional on-off microvalves are too expensive to be used for single-use biochip devices. We developed a valving mechanism in which paraffin is used as an actuator material that undergoes solid-liquid-phase transition in response to changes in temperature. Several one-shot valving schemes, including “close-open” and “open-close-open” valves (Figure 2), are demonstrated. The planar designs of these microvalves result in ease of fabrication and integration. Fluidic experiments showed that the paraffin-based microvalves have zero leakage in a “closed” position and a maximum hold-up pressure of 40 psi. The paraffin-based valves are robust and exhibit excellent mechanical stability. The response time required to open

and close the paraffin-based valves is on the order of 10 s. Successful DNA amplification in the PCR chamber gated by paraffin-based microvalves (Figure 2F) suggested that paraffin is compatible with PCR.

The planar designs of the paraffin-based valves do not include a flexible diaphragm and thus are simpler than traditional actuator/diaphragm designs that require multilayer structures. Although we have only demonstrated one-shot close-open and open-close-open valving schemes, other configurations can be easily achieved. For example, a toggle valve that consists of a number of open-close-open segments operated in sequence can perform a number of open-close cycles as designated. Although the time response ( $\sim 10$  s) of the paraffin-based microvalves is relatively slow as compared to that of many conventional microvalves ( $\sim$ ms), the paraffin-based valves have proven to be practical and useful in our biochip device where rapid response is not critical. It is believed that the time response could be improved by employing a paraffin material with a lower melting temperature. The fabrication process of the paraffin valves is compatible with many other material fabrication processes (such as Si, plastic, etc.). The precise loading of paraffin material (melted volume on the order of pL) into the microchannel to form a microvalve can be achieved using a wax injector (Microdrop GmbH), leading to a simple manufacturing method to implement them into complex microfluidic devices. This process can be much simpler than bulk processes (e.g., bulk etching of Si wafers), surface processes (e.g., thin-film processes), or chemical reactions (e.g., in situ polymerization<sup>16,37</sup>) used in more traditional valve approaches. Since paraffin is a commonly used and inexpensive material, the paraffin-based microvalves are cost-effective and highly desirable for many single-use and disposable microfluidic applications. It is worth

(33) Zdeblick, M. J.; Anderson, R.; Jankowski, J.; Kline-Schoder, B.; Christel, L.; Miles, R.; Weber, W., Hilton Head, SC, June 13–16, 1994, 1994; pp 251–255.

(34) Jerman, H. J. *Micromech. Microeng.* **1994**, *4*, 210–216.

(35) Barth, P. W.; Beatty, C. C.; Field, L. A.; Baker, J. W.; Gordon, G. B., Hilton Head, SC, June 13–16, 1994, 1994; pp 248–250.

(36) Ray, C. A.; Sloan, C. L.; Johnson, A. D.; Busch, J. D.; Petty, B. R. *Proc. Mater. Res. Soc. Symp.* **1992**, *276*, 161–166.

(37) Yu, C.; Mutlu, S.; Selvaganapathy, P.; Mastrangelo, C. H.; Svec, F.; Fréchet, J. M. J. *Anal. Chem.* **2003**, *75*, 1958–1961.

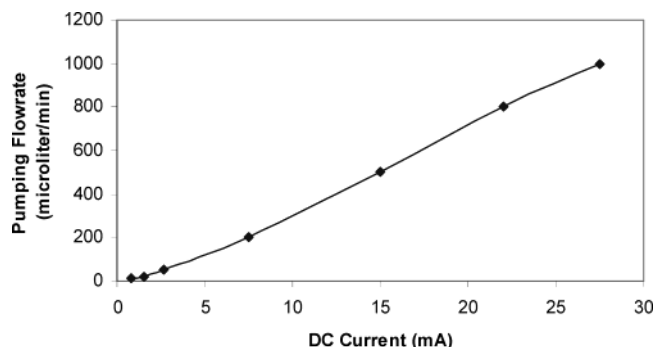


Figure 3. Measurement of the liquid pumping rate as a function of the applied dc current in an electrochemical pump that relies on the electrolysis of water between two platinum electrodes in a saline solution (20  $\mu$ L of 5 M NaCl).

noting that the valving approach is not limited to paraffin and can be extended to many other materials that can undergo a phase transition from solid to liquid in response to changes in temperature.

**Micropumps.** The biochip requires a transport of a wide range of sample volumes ( $\mu$ L–mL). Most conventional pressure-driven membrane-actuated micropumps<sup>38–40</sup> suffer from complicated designs, complicated fabrication, or high cost. In our device, two simple pressure-driven micropumping methods were employed: a thermopneumatic air pump (pump 4 in Figure 1A) for pumping of approximately microliter volumes, and electrochemical pumps (pumps 1–3 in Figure 1A) for approximately milliliter volumes. The former makes use of the air expansion in an air chamber, which is attached to a resistive heater in the PCB substrate, when heated. The air expansion is a nearly linear function of temperature. The resulting air expansion pushes the solution from the storage chamber into the downstream channels and chambers. The latter relies on electrolysis of water between two platinum electrodes in a saline solution to generate gases when a dc current is applied.<sup>41</sup> The gas generates a pressure that in turn moves liquid solutions in the biochip. Both pumping mechanisms do not require a membrane or check valves in their designs. As a result, their fabrication and operation are much simpler than most conventional micropumps. Flow experiments demonstrated that the thermopneumatic air pumps with air pockets of 50- $\mu$ L internal volume could efficiently move up to 60- $\mu$ L volume of fluids with a heater power consumption of less than 0.5 W. For pumping of approximately milliliter solution volumes, the electrochemical pump is more efficient and consumes less power. A steady flow rate of up to 0.8 mL/min was achieved with a power consumption of <150 mW (Figure 3).

**Pathogenic Bacteria Detection.** Pathogenic bacteria detection from a whole blood sample was performed using the described device. *E. coli* K12 cells inoculated in whole rabbit blood was used as a model for demonstration. Although this application may have no immediate practical use, it is easy to conceive a

system where, for example, the rabbit blood is replaced by human blood and pathogenic or cancer cells are targeted instead of the *E. coli* K12 cells. The *E. coli*/rabbit blood system was used because of the simplicity of performing the experiments as well as control assays in an ordinary laboratory setting (without BSL-2 or higher laboratory requirements).

The electrochemical signal corresponding to the hybridized *E. coli* K12-specific gene as shown in Figure 4A was obtained after 1-h hybridization. The whole analysis from loading the blood sample and different reagents into the storage chambers to obtaining the hybridization results took 3.5 h. The durations for the different operations are as follows: sample preparation 50 min, PCR amplification 90 min, pumping and valving 10 min, and hybridization 60 min. An on-chip assay from 1 mL of whole blood sample containing  $10^3$  *E. coli* K12 cells was also performed demonstrating positive recognition of the *E. coli* K12-specific gene but with low signal-to-noise ratio (data not shown here).

The typical cell capture efficiency using Dynabeads in our experiments is  $\sim 40\%$ . In the presence of  $1.3 \times 10^7$  (20  $\mu$ L) Dynabeads, the amplification efficiency was reduced by 50% as compared to the control PCR reaction performed without Dynabeads present (data not shown). It is believed that the chip assay sensitivity can be improved by assay optimizations, which include the following: (1) choice of smaller beads (100 nm in diameter as compared to 2.8  $\mu$ m for the M-280 Dynabeads) that can provide for higher cell capture efficiency due to increased surface-to-volume ratio;<sup>42</sup> and (2) use of paramagnetic beads with lower PCR inhibition rate as compared to the M-280 Dynabeads.

**Single-Nucleotide Polymorphism Assay.** In the hematocritosis-associated single-nucleotide polymorphism assay performed in our integrated device, the rare target capture and preconcentration steps were omitted since PCR amplification was performed directly from diluted blood samples.<sup>43,44</sup> Thermal cell lysis followed by an asymmetric PCR amplification was performed to amplify DNA sequences containing the sites for HFE-C polymorphism. After PCR, the hybridization buffer and the amplification product were pumped into the microarray chamber, followed by 1-h hybridization and electrochemical signal scanning. Genotyping result is shown in Figure 4B. The whole analysis from loading the blood sample and different reagents on the chip to obtaining the genotyping results took 2.7 h: cell thermal lysis/PCR 90 min, pumping and valving 10 min, and hybridization 60 min.

The integrated biochip device performs automated DNA analysis from complex sample fluids providing a step toward fulfilling the promise of rapid, automated genetic analysis in handheld devices. Although other attempts have been made in the past to integrate genetic amplification with detection, none of those approaches has addressed the difficult task of sample preparation with rare cell capture capabilities. The main purpose of on-chip sample preparation in an integrated diagnostic device described here is to enrich rare target cells from a large-volume clinical or environmental sample. Considering that the blood sample is a highly heterogeneous cellular and genetic medium (for example, 1 mL of whole blood contains  $\sim 10^6$  white blood cells,  $\sim 10^9$  red

(38) Su, Y. C.; Lin, L. W.; Pisano, A. P. *J. Microelectromech. Syst.* **2002**, *11*, 736–742.

(39) Zengerle, R.; Skluge, S.; Richter, M.; Richter, A. *Sens. Actuators, A* **1995**, *50*, 81–86.

(40) Unger, M. A.; Chou, H.; Thorsen, T.; Scherer, A.; Quake, S. R. *Science* **2000**, *288*, 113–116.

(41) Bohm, S.; Olthuis, W.; Bergveld, P. J. *Biomed. Microdevices* **1999**, *1* (2), 121–130.

(42) Ward, M. D.; Quan, J.; Grodzinski, P. *Eur. Cell. Mater. J.* **2002**, *3*, 123–125.

(43) Burckhardt, J. *PCR-Methods. Appl.* **1994**, *3*, 239–243.

(44) Panaccio, M.; Georges, M.; Lew, A. M. *Biotechniques* **1993**, *14*, 238–240.



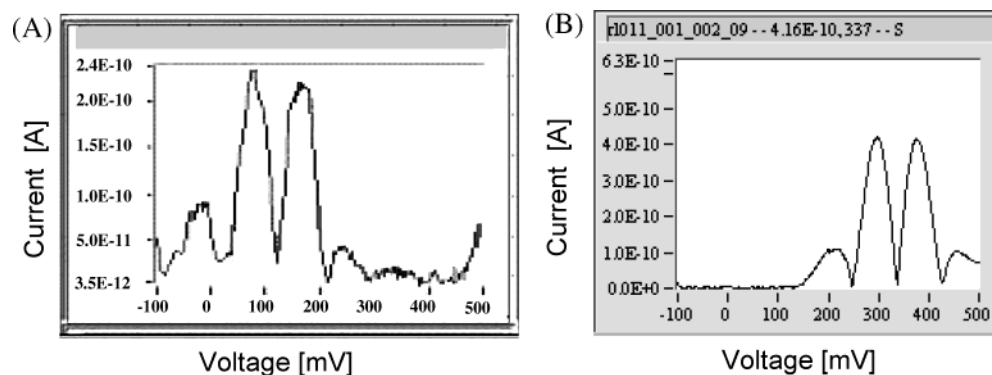


Figure 4. Electrochemical measurement results obtained from the integrated biochips. (A) Detection of  $10^6$  *E. coli* K12 cells from 1 mL of rabbit blood. (B) Genotyping identification of HFE-C gene from 1.4  $\mu$ L of human blood. During the hybridization process, alternating current voltammetry was used to detect the surface-bound redox molecules attached to the secondary probes. Fourier transformation was applied to the signal, and the fourth harmonic of the transformation, together with the redox current value, was displayed on screen.

blood cells, and  $10^7$  platelets, in addition to the serum components), a highly selective and sensitive target preconcentration poses a real challenge for on-chip integration of sample preparation steps. The use of immunomagnetic separation techniques for this purpose has a number of advantages, including high selectivity, ease of implementation, and reduced assay complexity, as compared to other approaches.<sup>3,5,45,46</sup> Moreover, the immunomagnetic approach allows for sample preparation and PCR amplification to be performed in the same chamber, which not only simplifies the device design, fabrication, and operation but also eliminates sample loss due to unnecessary fluid transfer. In the self-contained, integrated biochip system reported here, we have successfully demonstrated capturing  $10^6$  *E. coli* cells (equivalent to 5 ng of genomic material) from 1 mL of whole blood using the immunomagnetic beads separation technique. Further optimization, including fabrication of the device chamber to decrease the surface-to-volume ratio, choice of smaller beads system to increase the total surface area for target binding, and modification of PCR conditions for optimum amplification, would lead to the improvement of the assay performance and sensitivity. Other integrated devices demonstrated in the past used capillary electrophoresis<sup>10,14,47</sup> or real-time PCR approaches<sup>48</sup> as detection technologies. The CE technique does not provide information on the fragment sequence that is available through the use of PCR or hybridization methods. Multiplexing using real-time PCR is challenging since a maximum of four different fluorescent markers has been employed to date in a microchip. This only allows a 4-plex limit for the number of single-nucleotide polymorphisms that can be identified at a time.<sup>49</sup> Unlike CE and real-time PCR approaches, our electrochemical microarray detection provides a solution for highly multiplexed DNA analysis<sup>50,25</sup> with the capability of processing a complex, heterogeneous sample (i.e., PCR product containing denatured blood). Although the sensitivity of the electro-

chemical detection is in general lower than the optical detection techniques, the use of PCR to achieve sufficient concentration of DNA targets compensates for this drawback. The ability of our system to successfully perform genotyping with as little as 1.4  $\mu$ L of blood (corresponding to  $\sim 10\,000$  white blood cells) demonstrates its utility for clinical diagnostic applications. Moreover, the electrochemical detection system provides excellent specificity because of the usage of a "sandwich" assay.<sup>25</sup> Since our detection system can measure real-time hybridization without the need of a washing step, the assay can be terminated once the genotype is called by the instrument, saving valuable time. Furthermore, the assay performed in our biochip is flexible and has broad applicability due to this system proficiency in detection of both high-abundance and low-abundance DNA from complex biological samples.

The key microfluidic components in the biochip device, including paraffin-based microvalves, cavitation microstreaming mixers, and electrochemical pumps, are simple in design, inexpensive, and easy to fabricate and integrate into a complex microfluidic system, as compared with most of the existing microvalves, micromixers, and micropumps. The use of a cavitation microstreaming technique to achieve rapid and homogeneous on-chip microfluidic mixing not only increases the target cell capture efficiency in the sample preparation process but also allows hybridization assays to be performed in less than one-third of the time normally needed without mixing enhancement. The use of integrated microfluidic components with low power consumption, along with the employment of the electrochemical microarray detection, suggests that handheld operation is feasible for the device. The choice of inexpensive, robust microfluidic technologies, coupled with plastic chip fabrication and standard PCB process, facilitates an easy commercialization path for this technology. Although technical challenges remain, including increasing cell capture efficiency, detection sensitivity, and assay optimization, the platform shown here provides a solution for genetic analysis of complex biological fluidic samples in the fields of point-of-care genetic analysis and disease diagnosis.

(45) Wilding, P.; Kricka, L. J.; Cheng, J.; Hvichia, G.; Shoffner, M. A.; Fortina, P. *Anal. Biochem.* **1998**, *257*, 95–100.

(46) Cheng, J.; Kricka, L. J.; Sheldon, E. L.; Wilding, P. *Microsyst. Technol. Chem. Life Sci.* **1998**, *194*, 215–231.

(47) Woolley, A. T.; Hadley, D.; Landre, P.; deMello, A. J.; Mathies, R. A.; Northrup, M. A. *Anal. Chem.* **1996**, *68*, 4081–4086.

(48) Ibrahim, M. S.; Lofts, R. S.; Jahrling, P. B.; Henchal, E. A.; Weedn, V. W.; Northrup, M. A.; Belgrader, P. *Anal. Chem.* **1998**, *70*, 2013–2017.

(49) Klein, D. *Trends Mol. Med.* **2002**, *8*, 257–260.

(50) Umek, R. M.; Lin, S. S.; Chen, Y. P.; Irvine, B.; Paulluconi, G.; Chan, V.; Chong, Y. C.; Cheung, L.; Vielmetter, J.; Farkas, D. H. *Mol. Diagn.* **2000**, *5*, 321–328.

## CONCLUSION

We have developed a self-contained disposable biochip for fully integrated genetic assays. The on-chip analysis started with the preparation process of a whole blood sample, which included magnetic bead-based target cell capture, cell preconcentration and purification, and cell lysis, followed by PCR amplification and electrochemical DNA microarray-based detection. Crude biological sample and reagent solutions were loaded into the device, while electrochemical signals corresponding to genetic information were the primary outputs. The chip design is capable of handling a large volume (mL) of initial sample to accommodate analysis of rare targets in the sample. The milliliter volumes were reduced 100-fold when the assay reached the DNA amplification stage. All microfluidic mixers, valves, and pumps are integrated on the chip

but use very simple and inexpensive approaches in order to reduce chip complexity. Both low-abundance and high-abundance DNA detections from blood samples were demonstrated using the devices.

## ACKNOWLEDGMENT

The authors thank Motorola Life Science for supplying the eSensor devices. This work has been sponsored in part by NIST ATP Contract 1999011104A and DARPA Contract MDA972-01-3-0001.

Received for review November 4, 2003. Accepted January 9, 2004.

AC0353029